



Project 040 Quantifying Uncertainties in Predicting Aircraft Noise in Real-world Scenarios

**The Pennsylvania State University
Purdue University**

Project Lead Investigator

Victor W. Sparrow
Director and United Technologies Corporation Professor of Acoustics
Graduate Program in Acoustics
The Pennsylvania State University
201 Applied Science Bldg.
University Park, PA 16802
+1 (814) 865-6364
vws1@psu.edu

University Participants

Pennsylvania State University

- P.I.: Victor W. Sparrow, United Technologies Corporation Professor of Acoustics
- Co-PI: Philip J. Morris, Boeing/A.D. Welliver Professor of Aerospace Engineering
- FAA Award Number: 13-C-AJFE-PSU, Amendment 32
- Period of Performance: August 7, 2017 through December 31, 2018
- Task(s):
Quantifying the effect of uncertainty in meteorological conditions on aircraft noise propagation using techniques demonstrated by Wilson et al. (2014)¹

Purdue University

- P.I.(s): Kai Ming Li, Professor of Mechanical Engineering
- FAA Award Number: 13-C-AJFE-PU, Amendment 20
- Period of Performance: August 7, 2017 through December 31, 2018
- Task(s):
 1. Validate the noise model capabilities of AEDT by comparing numerical results with field data
 2. Quantify uncertainties of both model prediction and measurement in trying to predict aircraft noise (or pattern of change) in real world

Project Funding Level

FAA funding to Penn State in 2017-2018 is \$110K. FAA funding to Purdue in 2017-2018 is \$90K.

Cost sharing this year for ASCENT Project 40 was from ANOTEC Engineering, Motril, Spain regarding the BANOERAC data set. An in-kind cost share of \$115K was provided to both Penn State and Purdue, for a cost share total of \$230K. The point of contact for this cost sharing is Nico van Oosten, nico@anotecengineering.com.

Additional cost sharing from Airbus is in negotiation for next year in ASCENT Project 40 with respect to the SILENCE-R data set. The primary point of contact for that proposed cost sharing is Pierre Lempereur, pierre.lempereur@airbus.com, and the technical contact is Sasha Zaporozhets, zap@nau.edu.ua, of National Aviation University, Ukraine.

Investigation Team

Pennsylvania State University
Victor W. Sparrow (PI)



Philip J. Morris (Co-PI)
Graduate Research Assistant Harshal Patankar

Purdue University

Kai Ming Li (PI)
Graduate Research Assistant Yiming Wang

Project Overview

The purpose of this project is to understand the uncertainty in the prediction of noise of aircraft. Many ways of calculating aircraft noise are available. Also many experimental datasets have been obtained to assess aircraft noise. ASCENT Project 40 is developing methods that could later be used in FAA tools for predicting aircraft noise. There are three goals for the work of the current year:

- (1) Extend the uncertainty methods of Wilson, et al. (2014) and other algorithms to realistic aircraft trajectories and meteorology in the atmosphere, and comparing the calculated results with field data already acquired in the Vancouver Airport Authority, BANOERAC, and SILENCE(R) databases (Penn State);
- (2) Validate the noise model capabilities of AEDT by comparing numerical results with field data (Purdue);
- (3) Quantify uncertainties of both model prediction and measurement in trying to predict aircraft noise in real world (Purdue).

In addition, a collaborative initiative with National Aviation University of Ukraine is continued and a new close cooperation with Georgia Tech on ASCENT Project 43 was initiated.

If successful, the ASCENT Project 40 research will develop methodologies that should be implemented in FAA tools for predicting aircraft noise in the presence of real world weather. By having more accurate and faster predictions and predictions that were verified with field data, the project will allow FAA to more accurately predict the potential noise impacts when making decisions regarding FAA federal actions, such as in the site-ing of new runways and implementing new landing approach and take-off patterns over populated areas.

This research aims to enhance the accuracy of AEDT through improved aircraft noise propagation modeling. This improvement is needed to support the evaluation and development of aircraft flight routes and procedures that could reduce community noise. These improvements will also facilitate the implementation of NextGen through improved characterization of the efficiency benefits it would deliver.

Task 1– Quantifying the Effect of Uncertainty in Meteorological Conditions on Aircraft Noise Propagation Using Techniques Demonstrated by Wilson et al. (2014)¹

Pennsylvania State University

Objective(s)

This research seeks to not only to validate current FAA/Volpe noise modeling capabilities by comparing with measurement data, but also to quantify uncertainties of both model prediction and measurement in trying to predict aircraft noise (or patterns or changes) in real world situations, particularly when meteorological conditions over various different time periods may affect prediction output. The research will (1) review and analyze available field measurement data for patterns that are influenced by the (change of) meteorological conditions; (2) identify sets of field data for specific scenarios that contain proper parameters/quality input values to validate the enhanced modeling capabilities; (3) use the enhanced modeling capabilities to understand the patterns identified in the field measurement data that are influenced by the (change of) meteorological conditions and (4) quantify uncertainties in predicting aircraft noise in real-world situations. In addition, a new collaborative initiative on aircraft noise propagation model validation is continuing with National Aviation University, Kiev, Ukraine.



Research Approach

Introduction

Accurate prediction of aircraft noise is necessary for complying with noise regulations and for planning infrastructure around airports. To address these needs, sophisticated noise propagation models which account for the aircraft state, complexities in the propagation path and the ground condition are being developed. This necessitates addressing how the uncertainties in inputs for these high-fidelity models affect the predicted noise levels. The work presented here focuses on the effect of uncertainties in the meteorological conditions on the aircraft noise levels as received near the ground. Typically, simplified meteorological profiles, such as homogeneous or constant gradient, are used as inputs to the noise propagation models. The variation in meteorological profiles away from the mean values needs to be accounted for, to arrive at better estimates of the noise levels.

Wilson et al. (2014)¹ have demonstrated an approach to quantify the effect of uncertainties for near-ground outdoor sound propagation using the method of expected values and stochastic sampling techniques. These techniques have also been successfully employed recently² to address the variability in wind turbine noise which occurs because of the changes in wind velocity and direction. The work presented here extends the methodology to the geometry of aircraft noise propagation and addresses the effect of meteorological uncertainties on aircraft noise propagation.

Problem description (Assumed meteorological conditions and sound speed profile)

For this work, the profiles of temperature and wind are assumed to be range-independent. For simplicity, the relative humidity is assumed to be both height-independent and range-independent. A linear temperature profile is assumed as given by Eqn. (40.1) where L is the lapse rate and z is the height from the ground. A logarithmic wind speed profile is assumed to represent the eastward wind speed $u(z)$ as given by Eqn. (40.3), where z_0 is the roughness length. The value of roughness length z_0 is set to 0.02 m which is a typical value for flat terrain covered with grass. The equivalent sound speed profile resulting from the assumed meteorological conditions is obtained by Eqn. (40.4) and Eqn. (40.5).

$$T(z) = T(z)|_{z=0} + Lz \quad (40.1)$$

$$c(z) = c_0 \sqrt{\frac{273.15 + T(z)}{T_0}} \quad \text{where, } c_0 = 331 \text{ m/s and } T_0 = 273.15 \quad (40.2)$$

$$u(z) = b \ln\left(\frac{z}{z_0} + 1\right) \quad (40.3)$$

$$c_{\text{eff}}(z) = c(z) + u(z) \quad (\text{for eastward propagation}) \quad (40.4)$$

$$c_{\text{eff}}(z) = c(z) - u(z) \quad (\text{for westward propagation}) \quad (40.5)$$

Table 1. Gaussian uncertainty in the meteorological parameters.

Parameter	Units	Mean (μ)	Std. deviation (σ)
Temperature at the ground $T(z) _{z=0}$	°C	-3	3.7
Lapse rate L	°C/km	-4	1.5
Parameter b in the wind profile	m/s	1.1	0.6
Relative humidity r_h	%	85	4.5

Instead of expressing the parameters representing the meteorological profiles (e.g. the lapse rate L) by their mean values, they are expressed as probability density functions i.e. distributions of values with varying probability of occurrence. For simplicity, the Gaussian function is assumed to describe the uncertainties. The mean values and the standard deviations describing the probability density functions for the meteorological parameters are given in Table 1. These values are estimates based on the six-hourly data measured in January 2011 (State College, PA, USA). Figure 1 shows the effective sound speed profile obtained with Eqn. (40.4) and Eqn. (40.5) for the mean values of the meteorological parameters.

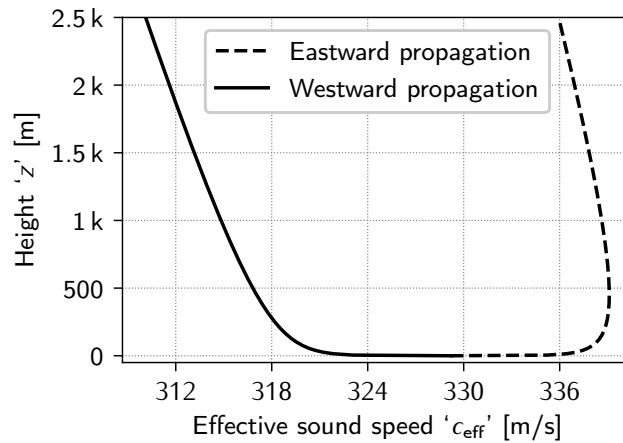


Figure 1. Effective sound speed profiles corresponding to the mean values of temperature and wind profiles.

Problem description (Source and receiver)

A retrofitted sound-power-level spectrum of a Boeing 777-300 (maximum thrust, departure setting)³ is used to represent an omni-directional source. The spectral content between 50 Hz to 2000 Hz is considered for calculations since higher frequencies are attenuated by atmospheric absorption and don't contribute significantly to the overall sound pressure levels. The sound power spectrum for one-third octave bands is shown in Figure 2.

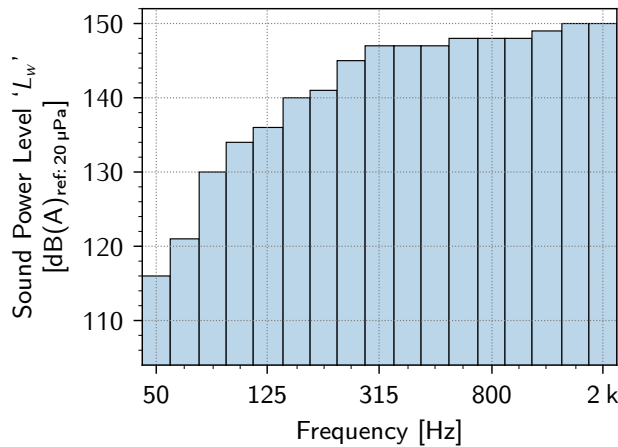


Figure 2. Retrofitted Boeing 777-300 sound power level spectrum (maximum thrust, departure setting)³

The receiver height z_r is set to 1.2 m and three different source heights z_s (1.0 km, 1.5 km, 2.0 km) are considered for the calculations. Propagation calculations are performed over a 10 km range (5 km each for eastward and westward propagation).

Problem description (Ground properties)

Attenborough's four-parameter model⁴ is used to represent a soft ground with static flow resistivity $\sigma = 200 \text{ kPa}\cdot\text{s}/\text{m}^2$, the porosity $\Omega = 0.27$, the grain shape factor $g = 0.5$ and the pore shape factor $s_f = 0.75$. The ground properties are assumed to be independent of the range.

Methodology (Approach for incorporating the effect of meteorological uncertainties)

Let $R[x, z_r, f, \phi_1, \dots, \phi_m]$ be the power spectral density [Pa^2/Hz] of the sound pressure level received at range x , receiver height z_r , the frequency f and for the meteorological variables ϕ_1, \dots, ϕ_m (such as lapse rate, temperature at the ground). If



the mean values of the meteorological variables are used as a representation of the reality, then Eqn. (40.6) would give the overall sound pressure level (SPL) at the receiver.

$$\Pi(x, z_r) = \int_{f_{\min}}^{f_{\max}} R[x, z_r, f, \underbrace{\phi_1, \dots, \phi_m}_{\text{mean values}}] df \quad (40.6)$$

The approach shown by Eqn. (40.6) neglects the deviations of meteorological variables from their mean values. It would be more realistic to use the expected value of the received SPL $\langle \Pi(x, z_r) \rangle$ which incorporates the effect of the uncertainties, as given by Eqn. (40.7).

$$\langle \Pi(x, z_r) \rangle = \int_{f_{\min}}^{f_{\max}} \int_{-\infty}^{\infty} \dots \int_{-\infty}^{\infty} R[x, z_r, f, \phi_1, \dots, \phi_m] g_{\phi_1}(\phi_1) \dots g_{\phi_m}(\phi_m) d\phi_1 \dots d\phi_m df \quad (40.7)$$

In Eqn. (40.7), ' $g_{\phi_1}(\phi_1), \dots, g_{\phi_m}(\phi_m)$ ' are the probability density functions (PDFs) for the uncertain variables ϕ_1, \dots, ϕ_m respectively. The uncertain variables are assumed to vary independently, hence their combined probability density function is equal to the product of the individual PDFs. It is clear from Eqn. (40.7) that adding more uncertain variables would imply more dimensions added to the integral for obtaining the expected SPL. An efficient approach to handle such multi-dimensional integrals is to use stochastic sampling techniques. To proceed with this approach, it is convenient to normalize the limits of integration. This is achieved by using normalized frequency ν as given by Eqn. (40.8) and cumulative density functions as given by Eqn. (40.9).

$$\nu = [\ln(f) - \ln(f_{\min})] / \Delta_f, \quad \text{where } \Delta_f = \ln(f_{\max}) - \ln(f_{\min}) \quad (40.8)$$

$$G_{\phi_m}(\phi_m) = \int_{-\infty}^{\phi_m} g_{\phi_m}(\phi_m) d\phi_m \quad (40.9)$$

After the change of variables, Eqn. (40.7) changes to Eqn. (40.10). After this, stochastic sampling techniques can be used to draw N random samples from each dimension of the integral and the integral is approximated as given by Eqn. (40.11).

$$\langle \Pi(x, z_r) \rangle = \int_0^1 \dots \int_0^1 R[x, z_r, f(\nu), \phi_1(G_{\phi_1}), \dots, \phi_m(G_{\phi_m})] f(\nu) \Delta_f dG_{\phi_1} \dots dG_{\phi_m} d\nu \quad (40.10)$$

$$\langle \Pi(x, z_r) \rangle \approx \frac{1}{N} \sum_{n=0}^{N-1} R[x, z_r, f(\nu_n), \phi_1(G_{\phi_1, n}), \dots, \phi_m(G_{\phi_m, n})] f(\nu_n) \Delta_f \quad (40.11)$$

It is important to note the interpretation of the presented mathematical procedure. Each random sample represents a set of values of all the uncertain variables and the frequency. The values for uncertain variables are drawn based on their cumulative density functions, which is an indirect way of applying the probability density functions. The advantage of this approach is that any method can be used for the propagation calculations.

Methodology (Wave propagation method)

In this work, a wide-angle Crank-Nicolson Parabolic Equation^{4,5} (CNPE) method is used as the propagation method. This method is chosen because it solves the exact one-way wave equation (neglecting back-scattering) and is accurate even for the low frequencies. The only caveat is that the angle limitation of CNPE restricts the usable numerical grid to elevation angles less than 35° as illustrated in Figure 3.

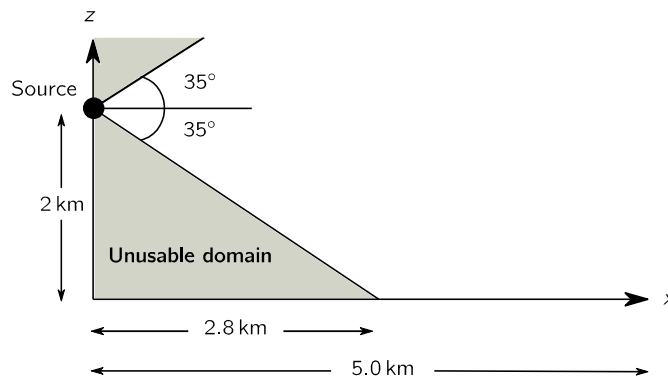


Figure 3. Angle limitation of CNPE method. Outside of the 35° elevation angle shown, the CNPE results are unreliable and such results are not included in the analysis.

Methodology (Atmospheric absorption)

This work assumes a rather simple approach to account for the attenuation due to atmospheric absorption. Attenuation due to atmospheric absorption is calculated using ISO 9613-1, based on (1) the value of relative humidity (which is allowed to vary), (2) the average temperature across the vertical profile (which varies with ground temperature and lapse rate), and (3) the geometric distance between the source and the receiver. For third-octave band calculations, the SAE-ARP-5534 method^{6,7} is used to correctly account for the absorption.

Numerical experiments

Using the methodology explained in the previous section, numerical experiments are performed for three different aircraft heights ($z_s = 1.0 \text{ km}, 1.5 \text{ km}, 2.0 \text{ km}$). For each aircraft height, four types of scenarios are considered i.e. (1) with no uncertainty in meteorological conditions (2) with uncertainty in temperature profile and relative humidity (3) with uncertainty in wind profile and (4) with uncertainty in temperature, wind profile and relative humidity. The results are shown in Figures.4 to 7.

Numerical experiments with no uncertainty in meteorological conditions are performed for 17 third-octave bands between 50 Hz and 2000 Hz. For numerical experiments which include the effect of uncertainties, 102 samples obtained using 'Latin Hypercube Sampling' (LHS) are used. The LHS method is chosen rather than the ordinary Monte-Carlo sampling since it has been shown¹ to be more accurate when the uncertainties involved are reducible (as is the case for this work). In general, it is challenging to determine the number of samples required to obtain accurate estimates using stochastic sampling techniques. The number of samples required does not necessarily depend on the number of uncertainties (since all the uncertain variables are handled simultaneously). It does depend on the sensitivity of the propagation calculation to the uncertain variables.

One way to check the accuracy of the estimated SPLs is to rely on confidence intervals obtained using the Bootstrap sampling method¹. But, the use of Bootstrap sampling requires large number of samples obtained using the ordinary Monte-Carlo sampling. Hence in this work, the accuracy of the estimated SPLs obtained using 102 LHS samples is checked by repeating the numerical experiments 10 times and calculating the RMS errors to see if they fall within acceptable limits (shown in Figure 7).

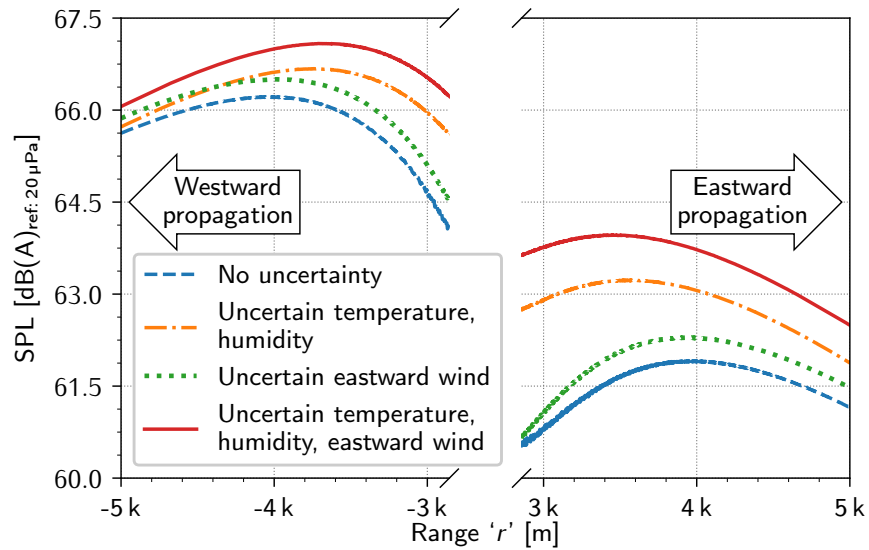


Figure 4. Effect of meteorological uncertainties on the received SPL for 2.0 km aircraft altitude. SPLs for eastward and westward propagation are shown on the right and left side of the plot respectively.

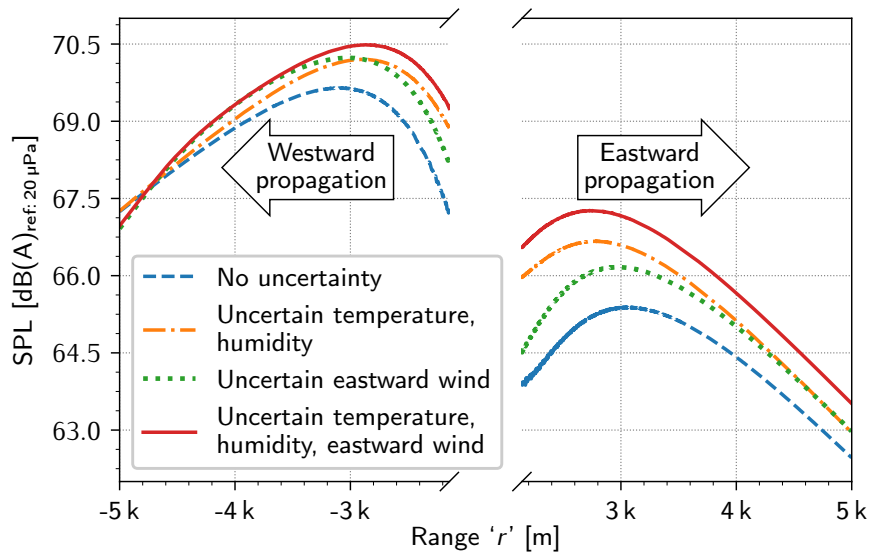


Figure 5. Effect of meteorological uncertainties on the received SPL for 1.5 km aircraft altitude. SPLs for eastward and westward propagation are shown on the right and left side of the plot respectively.

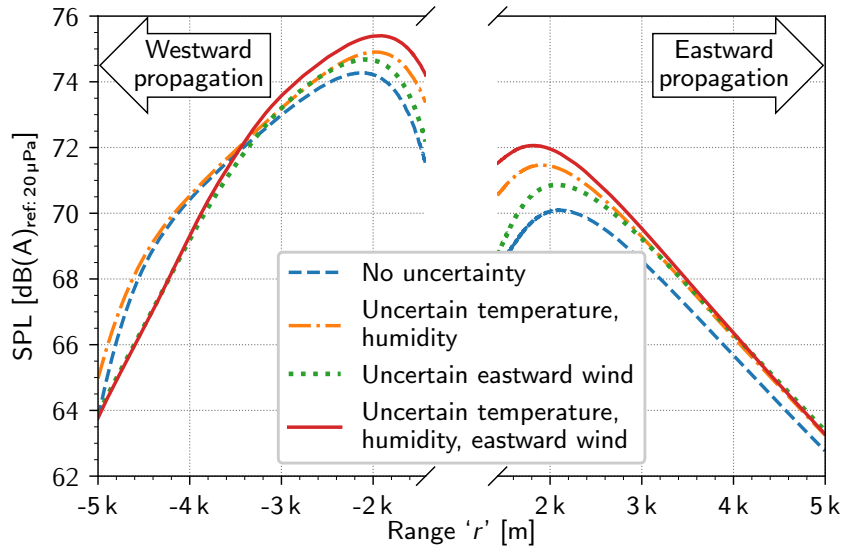


Figure 6. Effect of meteorological uncertainties on the received SPL for 1.0 km aircraft altitude. SPLs for eastward and westward propagation are shown on the right and left side of the plot respectively.

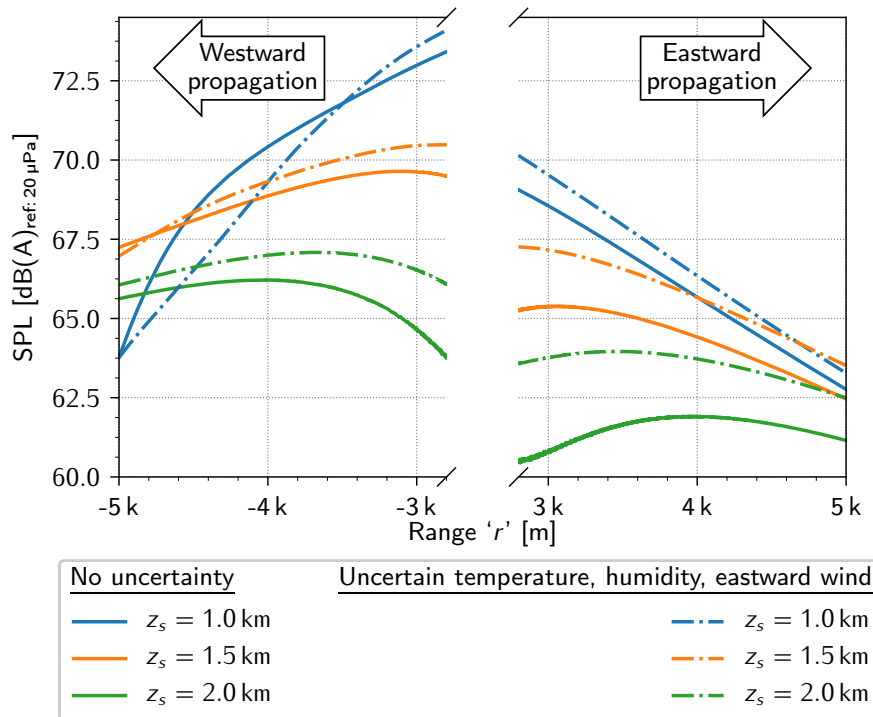


Figure 7. Effect of meteorological uncertainties on received SPLs for aircraft heights 1.0 km, 1.5 km, 2.0 km. Received SPLs for the no uncertainty cases are shown for comparison.

Results and discussion

- Looking at Figures 4 to 6, for a fixed source height, the effect of meteorological uncertainties seems to fade away as the distance between the source and the receiver is increased. This might be attributed atmospheric absorption, which increases with propagation distance and dominates over the effect of uncertainties. An exception to this observation can be seen for the westward propagation scenario. In the case of westward propagation, the effect of temperature lapse and wind adds up resulting in stronger upward refraction (see Fig. (40.1)). When the source height is lowered, upward refraction starts to play a noticeable role (e.g. around 3.5 km westward propagation for aircraft height 1.0 km as seen in Fig. (40.6)).
- Uncertainty in the wind profile alone seems to have a lesser effect on the received SPL when compared to the effect of uncertainty in temperature and humidity profile.
- Figure 7 shows the comparison of results obtained for three different aircraft heights (1.0 km, 1.5 km, 2.0 km) when all the meteorological uncertainties are considered simultaneously. It is evident that the effect of meteorological uncertainties is more pronounced when the source height is increased. This makes intuitive sense because increased source height implies a longer propagation path which allows for more exposure to the uncertainties in meteorological profiles.
- Figure 8 shows the RMS errors in the estimated SPLs (obtained by repeating the numerical experiments 10 times). It can be seen that the errors are less than 0.4 dB in all the cases. This implies that the estimations of the SPLs obtained using 102 LHS samples are reliable. The increase in RMS error for westward propagation in the case of $z_s = 1.0$ km can be attributed to the strong upward refraction (and its sensitivity to temperature and wind profile) as explained previously.

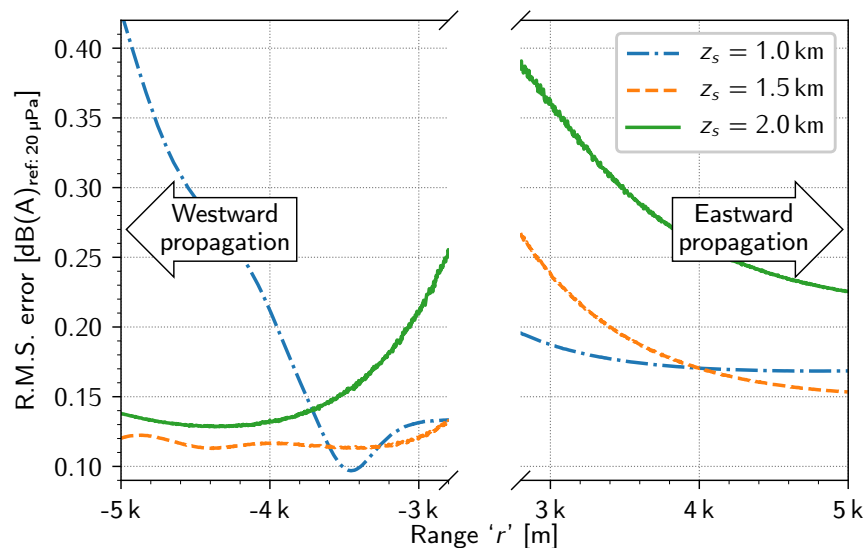


Figure 8. R.M.S. error in the estimation of SPL when uncertainties in temperature, humidity, wind are considered and 102 LHS samples are used. Since the RMS errors are below 0.4dB, the results obtained using 102 LHS samples are reliable.

Supporting investigations on source and directivity effects

Penn State also provided reviews and recommendations concerning the interpretation of the Discover A/Q acoustics data ongoing at Purdue University. In particular it was noted that the effects of source variation on the spiral flight paths could be minimized by taking data samples when the aircraft was travelling on a section of the flight path where it was normal to the observation station. If the source directivity is assumed to be symmetric about the aircraft, from port to starboard, then the differences in spectra, when allowance is made for the different propagation distances, should be dominated by propagation effects. Input was also provided on the likely directivity of a propeller-driven aircraft to assist in the choice of multipoles to be used in the source modeling.



Milestone(s)

The overall approach of Wilson et al. (2014)¹ has been shown to be adaptable for the aircraft noise prediction problem.

Major Accomplishments

One way of including uncertainty in aircraft noise sound level predictions has been successfully demonstrated. It is shown that the overall approach of Wilson et al. (2014)¹ is adaptable for the aircraft noise prediction problem. In the cases examined with the three uncertain variables of temperature profile, wind profile, and humidity, the expected values of sound pressure level change due to the uncertainty. The expected SPLs change since the variation around the mean input variables do not result in symmetric changes in the SPLs. Further, it was found that the uncertainty grows with increasing aircraft altitude, which is an expected result.

Publications

Patankar, H. P., and Sparrow, V. W. "Quantifying the effect of uncertainty in meteorological conditions on aircraft noise propagation." 47th International Congress and Exposition on Noise Control Engineering, INTER-NOISE 2018.

Outreach Efforts

None

Awards

None

Student Involvement

Graduate Research Assistant Harshal Patankar has been the primary person working on this task.

Plans for Next Period

1. In the work performed until now, the CNPE has been used for the propagation calculations. However, one can use any propagation method with the approach of Wilson et al. (2014)¹. A logical next step would be to determine if ray tracing and/or integrated calculation methods give similar results to the CNPE results if uncertainty is similarly included (as has been shown in the work presented in this report).
2. In the work completed thus far, a simple meteorological model of temperature lapse and logarithmic wind profile is assumed which could be replaced by a custom function fitted to measured atmospheric profiles. For now, the uncertainties have been modeled using Gaussian distribution for simplicity. In a real-world situation, the uncertainties might not be symmetrically distributed around their mean values (as in the case of Gaussian function), hence it would be better to build a custom probability density function based on measured atmospheric profiles.
3. Advanced stochastic sampling techniques such as importance sampling and adaptive importance sampling¹ could be used to reduce the computation time.

References

1. D. K. Wilson, C. L. Pettit, V. E. Ostashev, and S. N. Vecherin, "Description and quantification of uncertainty in outdoor sound propagation calculations," *The Journal of the Acoustical Society of America* 136(3), 1013-1028 (2014).
2. K. Poulain, "Numerical propagation of aircraft en route noise," Master's thesis, The Pennsylvania State University (2011).
3. E. M. Salomons, *Computational atmospheric acoustics* (Springer Science and Business Media, 2012).
4. M. West, K. Gilbert, and R. Sack, "A tutorial on the parabolic equation (PE) model used for long range sound propagation in the atmosphere," *Applied Acoustics* 37(1), 31-49 (1992).
5. E. J. Rickley, G. G. Fleming, and C. J. Roof, "Simplified procedure for computing the absorption of sound by the atmosphere," *Noise Control Engineering Journal* 55(6), 482-494 (2007).
6. "Aerospace Recommended Practice 5534: Application of pure-tone atmospheric absorption losses to one-third octave-band data," SAE Technical Report, SAE International (Issued8/2013).
7. Patankar, H. P., and Sparrow, V. W. "Quantifying the effect of uncertainty in meteorological conditions on aircraft noise propagation." 47th International Congress and Exposition on Noise Control Engineering, INTER-NOISE 2018.

Task 1 – Validate the Noise Model Capabilities of AEDT by Comparing Numerical Results with Field Data

Task 2 – Quantify Uncertainties of Both Model Prediction and Measurement in Trying to Predict Aircraft Noise (or Pattern of Change) in Real World

Purdue University

Research Approach

Background

Predictions of noise generated by en-route aircraft have become increasingly important in the current regulations on civil aviation worldwide.⁸⁻¹⁰ The propagation of airborne noise is influenced by many factors including the divergence effect, air absorption, acoustic impedance of the ground surfaces, effects of atmospheric refraction due to the presence of wind and temperature profiles, atmospheric turbulence and the aircraft's Doppler effect.¹¹ The Doppler effect perceived by a ground-borne receiver, which is caused by the motion of sound sources, will change two aspects of the aircraft noise. First, the received noise levels are augmented when an aircraft approaches and they are diminished for a receding aircraft. In the past, this effect has been studied extensively with theoretical modeling¹² and experimental measurements.¹³ Secondly, the perceived sound frequency at the receiver location will be shifted due to the motion of the aircraft. This apparent change in frequency depends on the aircraft's speed and the relative positions between the source and receiver. Although it cannot change directly the sound pressure levels, this Dopplerized frequency changes the characteristics of the received noise spectrum affecting human's perceptions. Generally speaking, noise sources with low pitch components (below 250 Hz, say) has shown less effect on annoyance than those with higher frequency (above 1000 Hz) components.

Some of the previous studies exploited the Doppler effect for tracking of aircrafts¹⁴, while other studies included it in their respective numerical models for synthesis of aircraft noise.^{15,16} We examine the influence of the Doppler shift on predicting en-route aircraft noise. Particularly, we investigate into the impact of the Dopplerized frequencies on the prediction of A-weighted noise levels due to an aircraft mounted with (a) jet engines or (b) turboprop propulsion systems.

The ray model used that provides a framework for calculating the attenuations due to geometrical spreading, air absorption and Doppler effect. Numerical simulations are presented quantifying the possible errors if the Doppler effect is not included in the prediction of the A-weighted sound pressure levels. Based on the ray model, the sound exposure levels for 89 spectral classes of flight arrival and departure data (obtainable from Ref. 8 and 24) are calculated with and without the inclusion the Doppler effects. The errors for not including the Doppler effect in the ray model are summarized in a bar chart for ease of reference.

1. Numerical simulations for flyover events

Despite its well-known shortcomings,²² A-weighted sound pressure level has become one of the internationally accepted metrics for evaluating aircraft noise. In this section, the ray model is applied to simulate the en-route aircraft noise. Specifically, the impact of the Doppler effect on the A-weighted noise levels is examined. Two distinct types of aircraft noise spectra are used in the numerical simulations:

- (a) Test aircraft: Lockheed P3B Orion mounted with turboprop engines;²¹
- (b) Reference aircraft: Lockheed Martin F22/A Raptors operating with the afterburners during the statics tests.²³

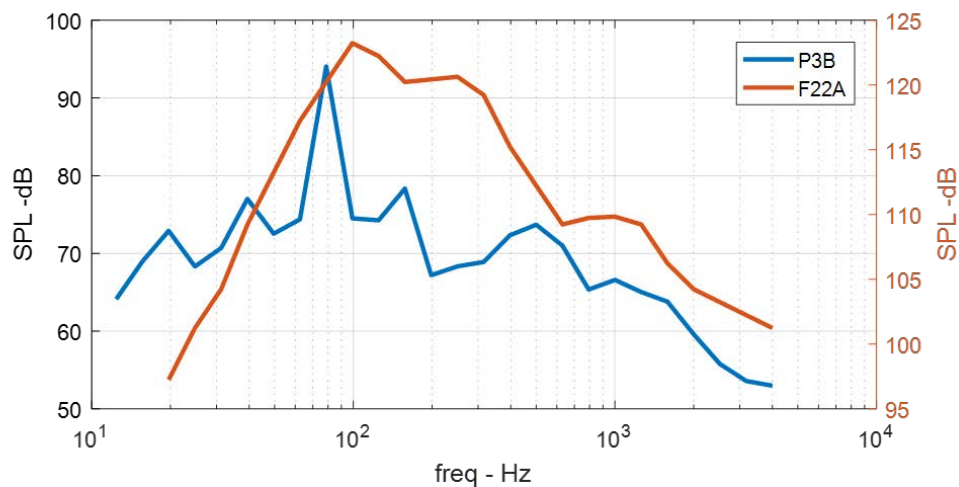


Figure 9. Measured spectra of sound pressure level (SPL) for Lockheed P3B Orion (blue) and Lockheed Raptor (red).

The scale of SPL for P3-B Orion is shown on the left vertical axis and Lockheed F22/A shown on the right axis. Here, the source directivity effects are not included in this study. Hence, one typical set of the source spectrum from each aircraft is used in our numerical simulations because the main objective of the present study is to examine the Doppler effect for a moving aircraft. In Figure 9, the spectrum of the P3-B Orion is shown in blue with the scale of the measured SPL displayed in the left vertical axis. For ease of comparison, the spectrum for the F22/A Raptor (with the scale of the measured SPL shown in the right axis) is plotted in the red line. As shown in Figure 9, the turboprop engine has a peak tonal component at about 70 Hz. On the other hand, the jet engine has demonstrated a broadband spectrum with the peak at about 100 Hz. The majority of the sound energy is concentrated between 50 and 500 Hz where the sound pressure levels dropped by 10 dB from about 123 dB at the peak to 113 dB at either sides of the limit. These two spectra are scaled in Figure 9 with the non-linear effects of jet engines ignored. These graphs represent the corresponding situations of obtaining the source spectra with each engine measured at 100 m from the source.

In the numerical analyses, the flyover of the P3-B Orion and the F22/A Raptor are simulated with the receiver located at 1 m above the ground. The numerical simulations are prepared with the aircraft traveling at a speed of approximately 100 m s⁻¹ (Mach number of 0.3) at a constant height of 500 m above the ground. The flight path has no offset distance between the aircraft and the receiver, i.e. a direct overhead flight path. The spectrograms for these two distinct engines are presented in Figure 10 in order to illustrate the effects of spectral characteristics upon the predicted A-weighted noise levels.

An aircraft flyover event is one of the most common operations near airports. When an aircraft is approaching, a higher pitch sound is heard due to the Doppler effect. When an aircraft recedes, a lower pitch sound is experienced instead. As a result, the frequency of the received sound is not exactly the same as that emitted by the aircraft due to the effect of Doppler shift. This section compares the possible error made by the Dopplerized frequency by comparing the effect on two different types of aircrafts: the P3-B Orion and the F22/A Raptor.

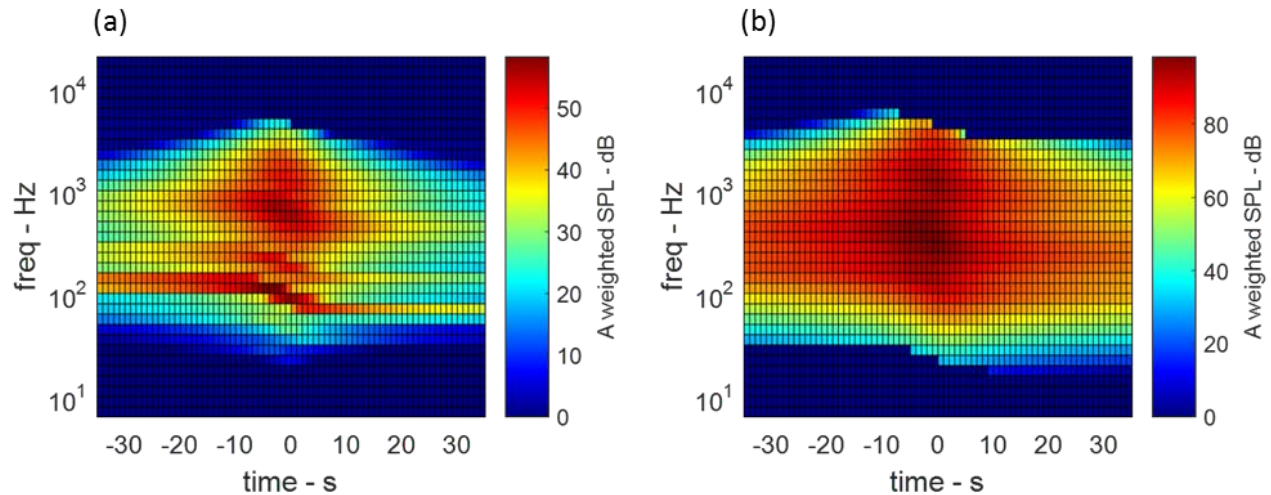


Figure 10. Predicted A-weighted spectrograms for (a) Lockheed P3-B Orion and (b) Lockheed Martin F22/A raptor (right). Flyover event with source height at 500 m and receiver height at 1 m, Mach number of 0.3 and sideline distance of 0 m.

As shown in Figure 9, the P3-B Orion has a clear tonal component around 70 Hz but the F22/A Raptor has a rather smooth broadband spectrum. The spectrograms in Figures 10 (a) and (b) show a clear Doppler effect especially for the P3-B Orion which has a dominant tonal component at 70 Hz. In the spectrograms, the one-third octave bands with the red/dark red colors have the highest sound pressure levels in the contour maps. When time is equal to zero, the aircraft is situated directly above the receiver. Increasing the time parameter from negative to zero (along the horizontal axis) indicates that the aircraft moves towards the receiver. The locations of the red color blocks moves towards the low frequency end as time increases in the spectrogram: this is mainly attributed to the effect of Doppler shift. Shifting in the frequency domain will cause the change in the predicted A-weighted SPL. A broadband and smooth source spectrum (such as that shown in the F22/A Raptor) has less noticeable frequency shift in the spectrogram, see Figure 10(b).

In Figure 11, the prediction of the A-weighted noise levels with and without the inclusion of the Doppler effect are compared. The predicted A weighted SPL with the Doppler effect is larger when the aircraft is approaching the receiver. This difference becomes zero when the aircraft is directly above the receiver and continue to decrease to negative value when it traverses away from the receiver. The comparisons between Figures 11 (a) and (b) show that the impact of the Doppler shift on the P3-B Orion is larger than that on the F22/A Raptor. The reason for this difference mainly lies in the fact that the spectral characteristics of these two types of aircraft are fundamentally different. The spectrum of the P3-B Orion has a dominant low-frequency tonal component at 70 Hz. When the Dopplerized peak frequency is shifted from 70 Hz to 110 Hz, the A-weighted correction factor will be changed by a factor of 6 dB. Hence, the sound source with the same unweighted sound pressure level will be increased by 6 dB because of a larger change in the correction factor as required by A-weighting of the sound levels. On the other hand, the smooth feature of the F22/A Raptor's spectrum makes the shift in Dopplerized frequency much gentler. For example, the frequency shift will have no effect to a broadband white noise because the sound pressure level is the same anywhere in the frequency domain.

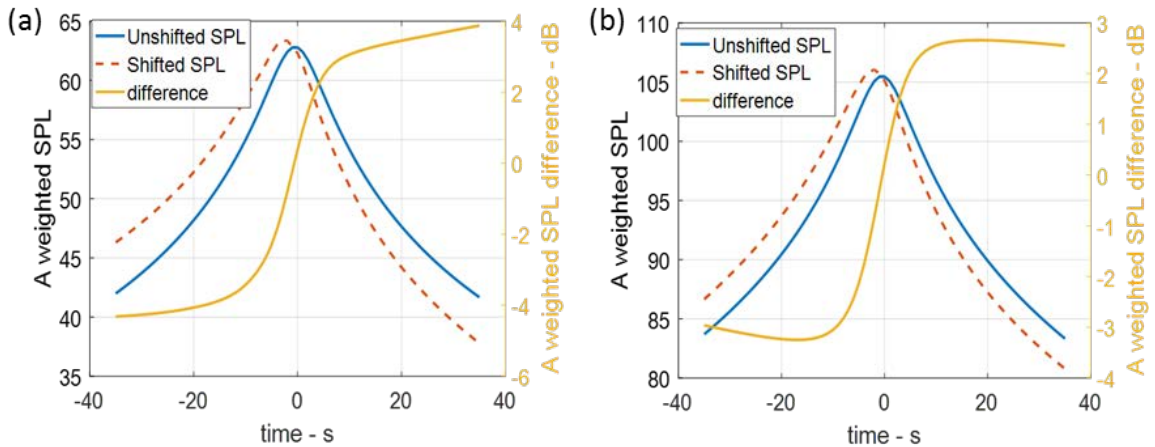


Figure 11. Predicted time histories of the overall A-weighted sound pressure levels (SPL). Blue line: Prediction without the Doppler effect. Red dashed line: Prediction with the Doppler effect. Yellow: Difference between these two predictions. (a) P3-B Orion; (b) F22/A Raptor.

Since the effect of the Doppler shift is decided by the spectral characteristics of the noise source, it is of interest to analyze this impact for different types of aircrafts with various spectral characteristics. In support of the current study, a dataset with 89 unique spectral classes have been used in Refs. 1 and 24 for assessing noise levels around airports.

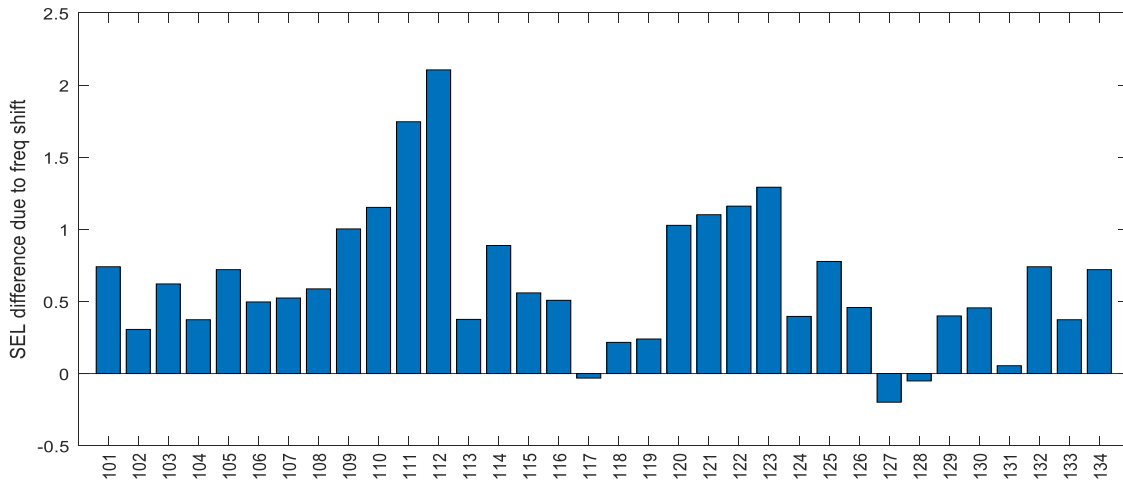


Figure 12. Difference in predicting A-weighted SEL with/without the inclusion of the frequency shift due to Doppler effect for the classes of flight departure.^{1,22}

Sound exposure level (SEL) is a widely used metric to evaluate the overall noise impact of a single fly-over event. According to the earlier explanations, different spectral characteristics tend to produce different results after the application of the Doppler shift to the ray model. Each of the 89 spectral classes are used as the source spectra in the prediction of SEL. Influence of the Doppler effect is not very prominent if SEL is used as the indicator. It is because the Doppler effect increases the noise levels of an approaching aircraft but it decreases the noise levels for a receding aircraft. These two influences are additive which leads to a partial cancellation when approaching and receding events are combined during the integration process in calculating the total SEL for a fly-over event.

Nevertheless, these 89 spectral classes are grouped into three categories: departure, arrival and flyover. For example, the class 101 represents the departure event of civilian aircraft Boeing 737. The detailed information of these spectral classes

can be found in Ref. 24. Only the results for departure and arrival classes are shown in this study for succinctness, see Figures 12 and 13 for the calculated results.

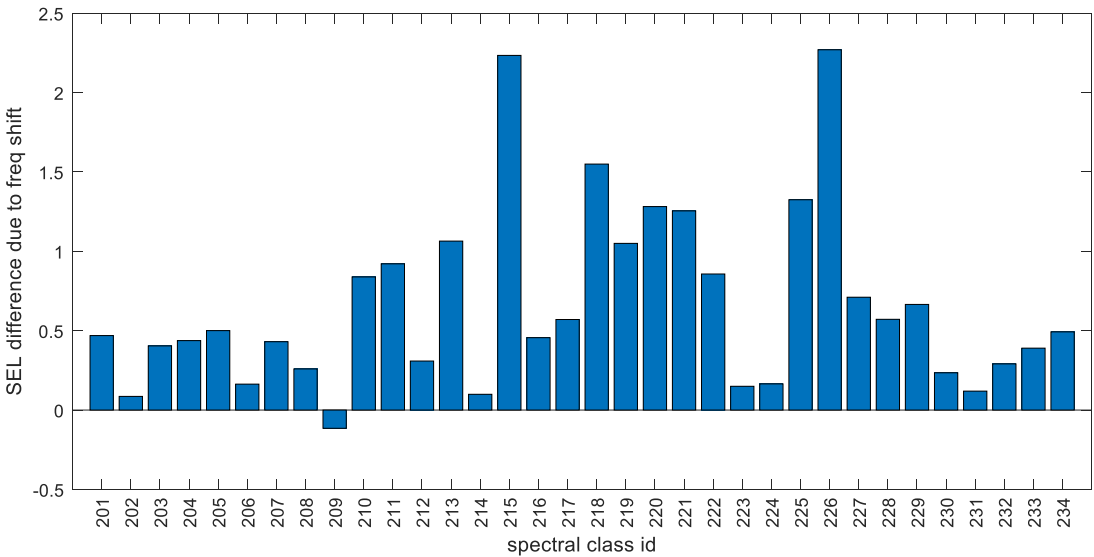


Figure 13. Difference in predicting A-weighted SEL with/without the inclusion of the frequency shift due to Doppler effect for the classes of flight arrival.^{1,22}

For the results presented in Figures 12 and 13, each of the spectra is used as the noise source in the prediction of SEL for a flyover event where 200 s before and after the overhead point are used in the numerical integration. The source and receiver heights are set, respectively, as 1 km and 1 m above ground and the source Mach number is set to 0.5. For the calculation of air absorption, the air temperature is set as 15° C, relative humidity as 50% and the atmospheric pressure ratio as 0.77. Using the ray model, the predicted SEL with and without the inclusion of the Doppler effect are compared.

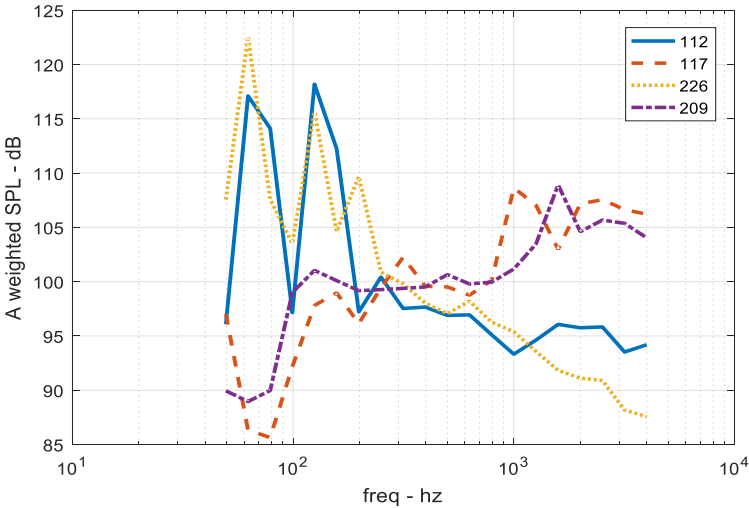


Figure 14. Source spectra for Classes 112, 117, 226 and 209.

With this set of calculations, the following conclusion can be drawn from the results shown in Figures 12 and 13. If the Doppler effect is not included in the SEL calculations, the possible ‘error’ varies between 0 and 2.2 dB for different classes of aircraft.



Among all spectra, classes 117 and 209 have the smallest influences caused by the effect of the Doppler shift. In contrast, classes 112 and 226 have the largest impacts. These 4 source spectra are organized and plotted in Figure 14 for illustration purposes. The two most influenced spectra have obvious tonal components with twin peaks at the spectral region around 100 Hz. The two least influenced spectra are relatively smooth. These 4 Spectral Classes confirm our observation in our earlier analyses for the P3-B Orion and the F22/A Raptor. A low-frequency tonal component can cause higher errors in the prediction of A-weighted sound pressure level if the Doppler effect is not included. On the other hand, an aircraft with a smooth spectral characteristic is less sensitive to the Doppler effect for accurate predictions of the A-weighted sound pressure levels.

Milestone(s) and Major Accomplishments

The Doppler effect on the prediction of the A-weighted sound pressure level is analyzed. The proposed ray model was validated with field data. The ray model was subsequently used to investigate the possible errors if the Doppler effect is not included in the prediction of A-weighted sound pressure levels. Numerical simulations were also conducted to calculate the sound exposure levels for 89 arrival and departure flight classes.¹⁷ It is found that an error exists between 0 to 2.2 dB if the Doppler effect is not included in the ray model. However, it is worth noting that noise predictions by the FAA's tool, the Aviation Environmental Design Tool (AEDT) is based on the Noise Power Distance (NPD) curves.¹ The NPD curves are typically developed by the aircraft manufacturers from measurement data. To a certain extent, the effect of Doppler shift is therefore captured in the current AEDT calculations. It may be useful to extend the analysis here to evaluate to what degree the Doppler effect is included in the NPD data.

Publications

- ASA Fall 2017, Abstract
- INTERNOISE 2018 paper

Outreach Efforts

None

Awards

Graduate Research Assistant, Yiming Wang has been awarded with INCE Best Graduate Student Award, 2018

Student Involvement

Graduate Research Assistant, Yiming Wang, has been the primary student working on this project. A new Graduate Research Assistant, Jianxiong Feng, has been recruited as Yiming Wang will be expected to finish his PhD thesis in the Summer 2019.

Plans for Next Period

For the Purdue effort, there are 4 tasks listed below:

- A. Assess the DISCOVER-AQ datasets for use in validating noise tools (propagation).
- B. Assess the influence of source (aircraft) motion on the accuracy in predicting en-route aircraft noise (source).
- C. Assess the impacts of geometric locations of source and receiver, the effective surface impedance and the ground topography on the accurate prediction of aircraft noise (receiver).
- D. Assess the overall uncertainty in the noise prediction (propagation+source+receiver) of overflight aircraft.

Three of these 4 tasks are conducted in coordination with the PSU team. The Purdue team will also focus on the use of DISCOVER-AQ datasets to investigate the influence of ground effects on predicting aircraft noise (Task C). Other Purdue efforts include the investigation of the Doppler Effect on the measured noise contents (for the shift in frequency and the change in the noise levels) for the approaching and receding aircraft.

References

8. Aviation Environmental Design Tool (AEDT) Technical Manual, Version 2d, US Department of Transport, Federal Aviation Administration, (2017).
9. ECAC.CEAC. Report on standard method of computing noise contours around civil aviation airports, Technical Report, ECAC.CEAC (2005).



10. Y. Wang, S. Liu, Y. Dong, J. Cai, "Effects of acoustic characteristics on annoyance of aircraft flyover noise," *Noise Control Engineering, Journal* **63**, 279-286 (2015).
11. B. G. Ferguson, Doppler effect for sound emitted by a moving airborne source and received by acoustic sensors located above and below the sea surface," *Journal of Acoustical Society of America* **94**, 3244-3247 (1993).
12. K. Attenborough, K. M. Li, and K. Horoshenkov. Predicting outdoor sound. CRC Press, (2014).
13. J. Lighthill, Introduction, Ch. 27, *Encyclopedia of Acoustics, Part III: Aeroacoustics and Atmospheric Sound*, pp 283-299, Wiley Online Library (1997).
14. S. R. Martin, M. Genesca, J. Romeu, T. Pamies, "Aircraft by means of the acoustical Doppler effect," *Aerospace Science and Technology* **28**, 305-314 (2013).
15. S. A. Rizzi, A. R. Aumann, L. C. Lopes, C. L. Burley, "Auralization of hybrid wing body aircraft flyover noise from system noise predictions," *Journal of Aircraft* **51**, 1914-1926 (2014).
16. M. Arntzen, D. G. Simons, "Modeling and synthesis of aircraft flyover noise," *Applied Acoustics*, **84**, 99-106 (2014).
17. Y. Wang, K. M. Li and B. N. Tong "Sound field generated by a 3-dimensional moving monopole point source above a locally reacting surface," *Noise-Con 2016*, Providence, RI, Paper 179. (2016).
18. B. N. Tong and K. M. Li. "Atmospheric effects on noise propagation from an en-route aircraft," *NOISE-CON 2014* nc-66594, Fort Lauderdale, Florida, September 8-10 (2014).
19. H. E. Bass et al, "Atmospheric absorption of sound: Further development." *Journal of Acoustical Society of America* **97**, 680-683, (1995).
20. International Standards Organization, "Acoustics - Attenuation of sound during propagation outdoors - Part 2: General method of calculation", International Organization for Standardization (1996).
21. E. Boeker et al, "DISCOVER-AQ Acoustics: Measurement and data report," DOT/FAA/AEE/2015-11 (2015).
22. Committee on Technology for a quieter America, National Academy of Sciences, "Technology for a quieter America," Ch. 3 Metrics for Assessing Environmental Noise. (2010) [see <https://www.nap.edu/read/12928/chapter/1> (Last assessed 1 May 2018)].
23. K. L. Gee et al, "The role of non-linear effects in the propagation of noise from high-power jet aircraft," *Journal of Acoustical Society of America*, **123**, 4082-4093 (2008).
24. H. He et al, "Integrated Noise Model (INM) Version 7.0 User's Guide," FAA-AEE-07-04, pp. 369-386 (2007).